

SBNCBS/NUP/96/01

Fluctuation dynamics and formation of exotic shape

S. Chattopadhyay¹

S.N. Bose National Centre for Basic Sciences, Block-JD, Sector 3, Salt Lake, Calcutta-700091, India

Abstract

To study the role of fluctuation in the collisional dynamics, Boltzmann- Langevin formalism is applied in a two dimensional scenario. The importance of collective flow towards the formation of hollow structure is exhibited in our simulation result. The observation of large clusters along the transverse direction indicates the non-equilibrium aspects of the fragmentation process in the late stage of the reaction.

PACS numbers : 21.65. +f, 24.60.Ky

¹e-mail : shila@tnp.saha.ernet.in

Numerical simulations based on Boltzmann-Ühling-Uhlenbeck (BUU) equation have been carried out extensively for intermediate energy heavy ion collision. These models have their origin in effective one body theories, happens to be very useful in understanding a wealth of nuclear properties [1]. The standard treatment (usually done in the Nördheim approach) takes into account only the average effect of the collision between the particles of the considered system. However, large scale fluctuation in density that manifests itself as fragments observed in the experiments cannot be described properly within the framework of single trajectory evolution of nuclear density. It is to be mentioned that owing to the presence of numerical noise one actually observes fluctuation in the solution of the BUU equation. This feature becomes very crucial when the di-nuclear complex passes the point of instability where any fluctuation whatsoever small can grow indefinitely. As a result the system may take any unphysical path in the trajectory variable space.

In this context, the stochastic transport models provide a more appropriate starting point. In the intermediate energy regime, noise associated with the two-body collision term is considered to be the dominant source of fluctuation. To retain this effect in the one body level within the framework of BUU equation different models [2] and several computational schemes following from these models have been proposed [3 - 6]. Accordingly, the one-body distribution function $f(\mathbf{r}, \mathbf{p})$ within an elementary cell around a point (\mathbf{r}, \mathbf{p}) of the related phase space of the system is considered to be the trajectory variable. A point along the trajectory is specified by the values of each $f(\mathbf{r}, \mathbf{p})$ over a given space of (\mathbf{r}, \mathbf{p}) at time t . To study the fluctuation around the deterministic *i.e.* the mean trajectory, the usual method is to incorporate fluctuating collision term in the BUU equation. The resultant equation for the evolution of phase space density is commonly known as Boltzmann- Langevin (BL) equation. Strictly speaking, for fermionic dynamics the value of the phase cell occupancy factor n_i (which differs from $f(\mathbf{r}, \mathbf{p})$ by a constant multiplicating factor $\Delta\mathbf{r}\Delta\mathbf{p}/h^D$, the phase cell volume in D dimensional physical space) takes a value either 1 or 0 . This feature automatically fulfills the relevant statistical relation related to the sample mean $\langle n \rangle$ and its variance $\sigma_i = \langle n \rangle_i \langle \bar{n} \rangle_i$. It is to be noted, however, that this feature does not allow us to make an attempt to produce correct magnitude of the noise by arbitrarily changing the phase cell occupancy within the samples from the known single or mean trajectory result calculated beforehand. In such cases, conservation principles related to the particle number, momentum and energy cannot be satisfied for every individual sample and dynamical correlation among the phase cell occupancies is completely lost. Therefore, the only possible option is to consider the evolution of each of the samples separately. Obeying the above mentioned criteria a novel simulation scheme is put forward for dynamical allocation of phase cell occupancy [6]. The simulation result reproduces the correct average behavior as compared with the mean trajectory result (in other words the solution of the BUU equation) for a test case where both of the results should be identical.

Most of the investigations so far done on the basis of BL model are mainly directed to study the

onset of clusterization in the nuclear matter situated inside the spinodal zone [7] which clearly shows the inadequacy of mean trajectory description of such catastrophic phenomenon. For this particular case, appropriate theoretical analysis has also been done for studying the growth of density fluctuation [8, 9] which in turn, provides an opportunity to check the reliability of the different simulation schemes. In this situation, fragments may appear anywhere within the volume with no significant spatial correlation. However, for a finite nuclear system the process of fragment formation may take place in a different manner. The standard mean trajectory calculation near Fermi energy domain explores the other alternatives [10]. Within a specific incident energy window of 50-100 MeV, the di-nuclear system takes exotic shapes due to the presence of instability and the fragments appear essentially by breaking of such structures. Later works have confirmed in a more rigorous manner such possibilities [11] even at lower collision energies [12]. This interesting observation promptly initiated some theoretical calculation to find out the experimental signatures of such facts [13], but there is still no conclusive experimental evidence [14]. From the theoretical point of view, when the issue is to study the dynamical evolution of the system in the presence of well developed instability, it seems more appropriate to probe the associated trajectory variable space around the mean path. This can be realized within the BL model by allowing the evolution of a given number of samples individually. Fluctuation appeared in this theory as a dynamical variable rather than as a numerical noise. This method thus serves to test the extent to which the mean trajectory calculation is reliable. With this notion, in the present work we study the dynamical evolution of the collision process in the trajectory variable space. However, our study is confined to the 2D physical space where some of the essential features of the dynamics of fragment formation can still be unraveled.

In the present study we consider the head-on collision between two identical spherical blobs in 2 dimension, each of them having rms radius of 5 fm. which is the same as that of the nucleus of mass number ≈ 100 . For the effective one body field we employ a simplified Skyrme interaction [15, 9]

$$U(x, y) = A \frac{\rho(x, y)}{\rho_0} + B \left(\frac{\rho(x, y)}{\rho_0} \right)^2 \quad (1)$$

with $A=-100.2$ and $B=48$ which correspond to the value of compressibility modulus $K = 288$ MeV and Coulomb interaction is included for protons. To evaluate effective potential on the co-ordinate grid, an averaging over 2D gaussian function of width 0.87 fm is considered. For the simulation on phase space lattice we use (27×27) cells in momentum space having width $\Delta p \approx 58$ MeV/c which covers the range ± 780 MeV/c in each of its direction and the corresponding cell width in co-ordinate space Δx is taken to be $\frac{1}{3}$ fm. Each filled phase cell can be considered as a particle. To describe nuclear matter at saturation density ρ_0 ($=0.55$ fm $^{-2}$) in a unit coordinate cell one needs 2×69 such particles such that a single nucleon is represented by nearly 2200 particle states for every sample. For an average description of the evolution we consider simulation of 20 such identical samples separately. In order to express the total energy of the di-nuclear system in the initial state as the sum of binding energies and the energy related to the boost,

the boost momentum should be chosen as a simple multiple of the grid width Δp_x only (say B_{fac}). This will also yield an accurate determination of the component of the flow velocity $\mathbf{u}(x, y)$ at every spatial cell initially and in subsequent time. In the present work the values of B_{fac} are taken to be 2, 3 and 4 which correspond to the values of incident energy E_{lab} 32, 68 and 117 MeV/nucleon, respectively.

The solution for the Vlasov part of the BUU equation is realized within our model by standard Leap-Frog routine similar to that used in ‘test-particle’ approach. (see ref.[9], for details). It is to be noted that due to the presence of fluctuating collision term, the symmetry in the coordinate as well as in the momentum space of the initial distribution is gradually lost. This feature may trigger a certain situation so that in the process of Vlasov propagation more than one particle may try to access the same phase cell. This disturbing feature is reduced substantially by simply choosing the time step of the simulation $\Delta t = m \frac{\Delta x}{\Delta p}$ (≈ 5 fm/c in our case) which is exactly the time needed for a particle to move at least one single step in the spatial grid. It is observed that in this collisional scenario the number of such events always happens to be less than even 10 for all values of B_{fac} mentioned above, whereas the total number of successful collisions may reach a value more than 40,000 in a single time step for an individual sample.

Let us concentrate on the simulation result of the collision between two identical blobs in 2D. We mainly discuss here the case related to the value of $E_{lab} = 68$ MeV/nucleon. The sample average density distribution $\rho(x, y)$ in units of ρ_0 is plotted in Fig. 1 for different stages of the collision. It is observed that within the time 30 fm/c the di-nuclear complex attains maximum compression. The central density reaches the value $\approx 1.6\rho_0$. After that, the matter flows radially outwards where the flow velocity along the transverse direction of the collision i.e. along y axis, is much higher than that along x axis. An interesting feature is observed during decompression at a time $t \approx 60$ fm/c. A narrow circular band appears near the periphery of the composite system (see Fig. 1(a)) and later on, matter deposits continuously around this band which makes it wider due to the outflow of the matter from the central region. This process continues until the central density drops down to a very low value which is even less than 5% resulting in the formation of a ring-like structure. However, the matter distribution along the ring is not uniform. Relatively stronger flow along y axis even at very late stage of the collision produces eventually much larger deposition of matter near y axis. The maximum density here attains a value of about $0.60\rho_0$ at $t = 200$ fm/c, and in other parts of the ring the average density takes the value $\approx 0.30\rho_0$. It is to be mentioned that the stability of this exotic shape depends crucially on the magnitude of the flow velocity. At a lower collision energy of $E_{lab} = 32$ MeV/nucleon, the structure does not expand much due to smaller values of flow velocities. Although we observe central rarefaction in the matter density which, however, is smeared out completely around the time 250 fm/c and a much elongated residue having uniform density of $0.8\rho_0$ is left.

From this study it is revealed that the appearance of the small band like structure or a notch in the density distribution at the earlier stage of the collision is the key feature which is instrumental in the

formation of exotic shape. In order to gain additional insight to its formation, we compute the diagonal components of the pressure tensor \mathbf{P} , the spatial gradient of which is essentially connected to the temporal variation of the flow velocity $\mathbf{u}(x, y, t)$. In Fig. 2 we plot the components $\langle P_{xx} \rangle$ and $\langle P_{yy} \rangle$ in the rest frame of the fluid along y axis which are computed by the appropriate relation as given below

$$\begin{aligned} P_{\alpha\beta}(x, y; t) &= \int (p_\alpha - \bar{p}_\alpha)(p_\beta - \bar{p}_\beta) f(x, y, p_x, p_y; t) d\mathbf{p} \\ &+ \delta_{\alpha\beta} \left(\frac{A}{2} \frac{\rho(x, y; t)}{\rho_0} + \frac{2}{3} B \left(\frac{\rho(x, y; t)}{\rho_0} \right)^2 \right) \rho(x, y; t) \end{aligned} \quad (2)$$

where $\bar{p}_\alpha = m u_\alpha$. As the reaction proceeds the pressure which initially is zero everywhere increases towards the center with the gradual piling up of matter there. Near the boundary, on the other hand, the low value of density may lead to a negative pressure. In general, the location of the minima of the pressure profile depends on the particular choice of the equation of state one uses for simulation. It is to be noted that due to the continuous outflow of matter and moreover, since pressure is zero at the vacuum, these points of minimum stay near the matter boundary until the density at the central region drops down substantially. Therefore, a pocket is formed as shown in the Fig. 2(a) where matter can accumulate or be trapped so that a band like structure appears in the density profile. with time this pocket moves outwards as the system expands. On the contrary, no such pocket is observed in the profile of P_{xx} along y direction (see Figs. 2(a) and 2(b)). The importance of asymmetry of the momentum distribution on the formation of this band may be understood from the differences in magnitude of P_{xx} and P_{yy} . To elaborate it further, we plot the the magnitude of $\langle Q(x, y) \rangle$ along y axis in Fig. 3 in accordance with the following definition

$$Q(x, y) = \frac{\int \left((p_x - \bar{p}_x)^2 - (p_y - \bar{p}_y)^2 \right) f(x, y, p_x, p_y) d\mathbf{p}}{\int \left((p_x - \bar{p}_x)^2 + (p_y - \bar{p}_y)^2 \right) f(x, y, p_x, p_y) d\mathbf{p}}. \quad (3)$$

. The magnitude of the flow velocity $\langle u_y(0, y) \rangle$ is also depicted in the same graph. The x component of the velocity u_x along y axis is found to be almost zero through out the evolution. The deposition of matter near the boundary means a negative slope to the flow velocity $\mathbf{u}(\mathbf{R})$ at these points which otherwise, is expected to be a rising function of the radius R [16]. The total landscape of $\langle Q \rangle(x, y)$ can be constructed from similar parallel curves as shown in Fig.3(a) and 3(b). Simultaneous attainment of high values of both the quantities $\langle u_y \rangle$ and $\langle Q \rangle$ imples the presence of collective flow (Figs. 3(a) and 3(b)). On the other hand, if such a high value of u_y is attained due to the collisions among particles only, then one should expect an opposite trend, *i.e.* the value of u_y then increases with decreasing value of Q . In spite of the fact that the matter flows outwards with very high velocities and moreover, near the boundary, its magnitude exceeds that of the local sound velocity, a rarefaction wave behind this shock proceeds towards the center. This feature is attributed to a certain amount of fluctuation in the spatial variation of P_{yy}

(see Fig. 3(c)). As a result, we observe a plateau in the landscape of flow velocity which in turn produces depletion of matter behind the shock. From the above analysis it appears that strong collective flow and also a specific behavior of Q that arises in the earlier stages of the collision, happens to be quite important for the formation of the hollow structure. We observe that equilibration attains earlier in the peripheral zone of the residue as seen from Fig. 3(d) and is also evident from Fig. 2(d). Due to this typical behavior of $Q(x, y)$ the process of the formation of hollow structure is now being hindered, which is also apparent from a closer look at the spatial variation of P_{xx} and P_{yy} in Figs. 2(d) and 2(e). This is probably the real cause why in low energies the structure ultimately collapses towards the center and the role of external force as produced by Coulomb interaction becomes important in later stages. Eventually, when the central density drops down substantially with respect to that near periphery so that the pressure at center becomes less negative, the process of the formation of structure becomes self-sustained. This feature is essentially connected to the very nature of the nuclear matter below subnormal densities as has already been pointed out in Ref. [16] and observed in our simulation (see Fig. 2(f)). Along the beam direction *i.e.* along the x axis, one observes a ‘stopping’ as the central density reaches its maximum value. However, at large x , matter still flows towards the center. At later times, due to the expansion, matter flows radially outward. The magnitude of the resultant of two opposing flow velocities along x axis is less than that along y direction. As a result, in course of time, the residue gets an elongated shape with larger deposition of matter along the transverse direction.

Another important aspect of the dynamics, the process of clusterization, can be accommodated in a proper manner within the present formalism. Although we observe considerable smoothness in sample averaged density, however, in the later stage of the collision large scale fluctuation in the density is present in an individual sample. After a time of ~ 100 fm/c when the overall density of the residue decreases down to a value of $\approx 0.4\rho_0$, the fluctuation becomes appreciable indicating the onset of clusterization. It is observed that $\delta\rho (= \sqrt{\sum(\rho_i - \langle \rho \rangle)^2})$ is nearly proportional to the density ρ itself. Therefore, the landscape of $\delta\rho(x, y)$ looks similar to that of ρ as shown in Figs. 1(b) and 1(c). However, the proportionality constant of $\delta\rho/\rho$ gradually increases with time and attains a value ~ 0.6 at a time $t=200$ fm/c. The wavelengths of the dominant unstable modes corresponding to the observed density fluctuation [4, 17] are much larger than the width of the ring formed as shown in Fig. 1(c). Therefore the finite size effect due to the relatively smaller width of the ring limits the role of spinodal instability in the fragment formation process. On the other hand, due to the continuous stretching along both y and x direction, the structure breaks-up into several fragments. This feature is exhibited in Fig. 4. Two large clusters along y direction are always present in each of the samples and along with it several small size clusters and elongated pre-clusters also appear like beads around the rim of the elongated ring. Similar features have been also observed at a higher incident energy of $E_{lab} = 117$ MeV/A. In this case, the average density at the final stage is quite low $\approx 0.20\rho_0$ and the density along y direction near the periphery is still higher attaining a

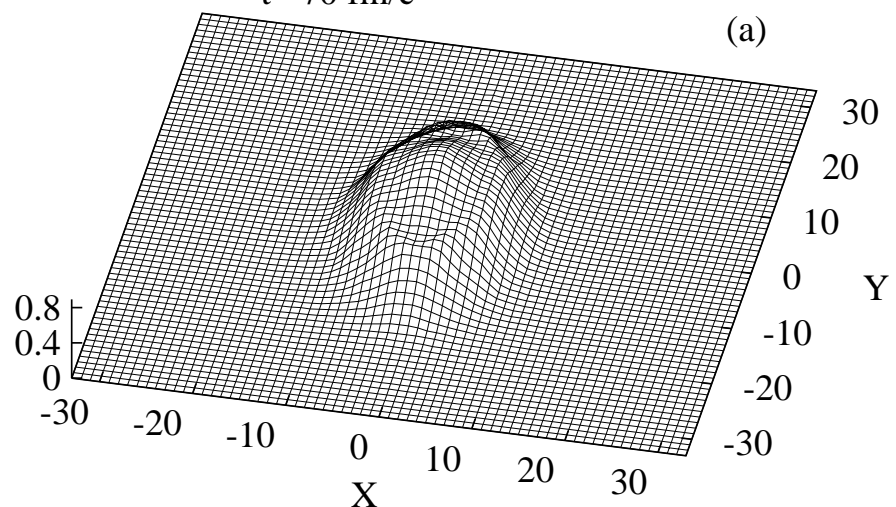
value of $\approx 0.4\rho_0$. It is to be noted that due to the faster rate of stretching here, arising from the relatively larger collective flow, the size of the clusters becomes very small which disappear gradually from the spatial grid. However, to check evaporation of matter from the surface of small clusters, the time step of the simulation at this stage should be decreased further. A better option is to use the standard Vlasov algorithm in the continuous space rather than in the lattice space so that time step can be chosen as small as required.

In conclusion, within the BL formalism a simulation study has been performed to investigate the dynamics of fragmentation process. In the less complicated scenario in two dimensions, we analyze the role of collective flow towards the formation of exotic shapes. It drives the system in such a manner so that the composite nuclear object along the trajectory can reach the saddle of the deformation energy and subsequently the system appears in a hollow shape. Because of the fact, that Pauli blocking effect is included properly within our simulation method and moreover, the representative particles obey proper statistical criteria, the freeze-out temperature of the residue can be determined accurately from sample average values of kinetic energy and number of particles at particular spatial grid. However, the observed fluctuation in ρ is larger than that associated to the temperature extracted from the average description. It is also interesting to note, that in spite of the presence of substantial amount of fluctuation in density at later stages of the collision, the related dynamics of the formation of structure is mainly controlled by the average description of the evolution. Therefore, we are still in the linear regime of the fluctuation dynamics. The history of the formation of structure or in other words, the entrance channel effect even persists in the process of fragmentation which is reflected by the production of large clusters along transverse direction. A proper 3D calculation along this line is called for to test the predictive power of this simulation scheme. By this means, it may be possible to assess the reliability of mean-field models based on semi-classical approaches for the description of nuclear fragmentation.

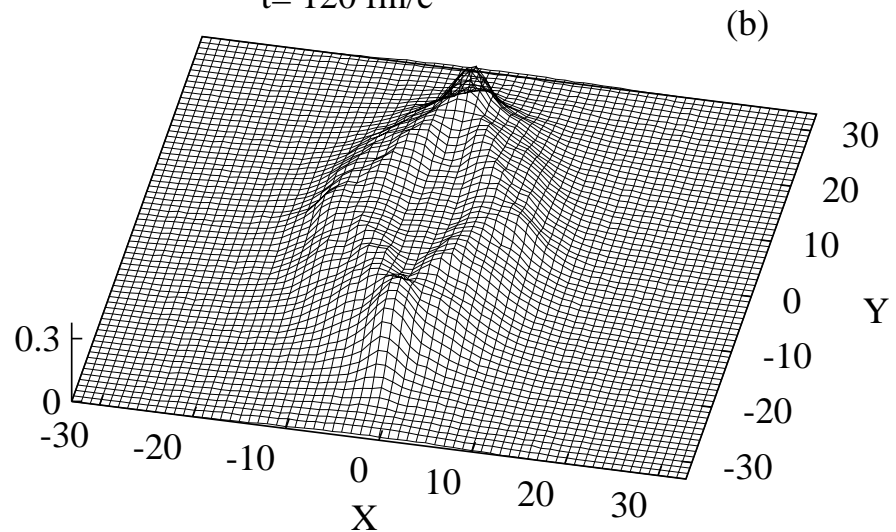
References

- [1] G.F. Bertsch and S. Dasgupta, Phys. Rep. **C160** 189 (1988); W Cassing, V. Metag, U. Mosel and K. Nita, Phys. Rep. **C188** 363 (1990).
- [2] S. Ayik and C. Gregoire, Nucl. Phys. **A513**, 187 (1990); J. Randrup and B. Remaud, *ibid.* **A514**, 339 (1990).
- [3] E. Suraud, S. Ayik, M. Belkacem and J. Stryjawska, Nucl. Phys. **A542**, 141 (1992).
- [4] G.F. Burgio, Ph. Chomaz and J. Randrup, Nucl. Phys. **A529**, 157 (1991).
- [5] M. Colonna, G.F. Burgio, Ph. Chomaz, M. Di Toro and J. Randrup, Phys. Rev. C **47**, 1395 (1993); G. F. Burgio, Ph. Chomaz and J. Randrup, Phys. Rev. Lett. **73**, 3512 (1994).
- [6] S. ChattoPadhyay, Phys. Rev. C **52**, R480 (1995).
- [7] G.F. Burgio, Ph. Chomaz and J. Randrup, Phys. Rev. Lett. **69**, 885 (1992).
- [8] M. Colonna, Ph. Chomaz and J. Randrup, Nucl. Phys. **A567**, 637 (1994).
- [9] S. ChattoPadhyay, Phys. Rev. C **53**, R1065 (1996).
- [10] L.G. Moretto, Kim Tso, N. Colonna and G.J. Wozniak, Phys. Rev. Lett. **69**, 1884 (1992); W. Bauer, G.F. Bertsch and H. Schulz, *ibid.*, 1888 (1992); D.H.E. Gross, Bao-An Li and A.R. DeAngelis, Ann. Phys. (Leipzig) **1**, 467 (1992).
- [11] H.M. Xu, C.A. Gagliardi, R.E. Tribble and C.Y. Wong, Nucl. Phys. **A569**, 575 (1994); Phys. Rev. C **49**, R1778 (1994).
- [12] B. Borderie, B. Remaud, M.F. Rivet and F. Sebille, Phys. Lett. B **314**, 265 (1993); B. Jouault, F. Sebille, G. Royer and V. de la Mota, Nucl. Phys. **591**, 497 (1995).
- [13] L. Phair, W. Bauer and C.K. Gelbke, Phys. Lett. B **314**, 271 (1993); T. Glasmacher, C.K. Gelbke and S. Pratt, *ibid.*, 265 (1993); Subrata Pal, S.K. Samaddar, A. Das and J.N. De, Phys. Lett. B **337**, 14 (1994).
- [14] M. Bruno *et al.*, Phys. Lett. B. **292**, 251 (1992); D.O. Handzy *et al.*, Phys. Rev. C **51**, 2237 (1995).
- [15] M. Colonna, M. Di Toro and A. Guernera, Nucl. Phys. **A580**, 312 (1994).
- [16] P. Danielewicz, Phys. Rev. C **51**, 716 (1995).
- [17] S. Ayik, M. Colonna and Ph. Chomaz, Phys. Lett. B **353**, 417 (1995).

$t = 70 \text{ fm}/c$



$t = 120 \text{ fm}/c$



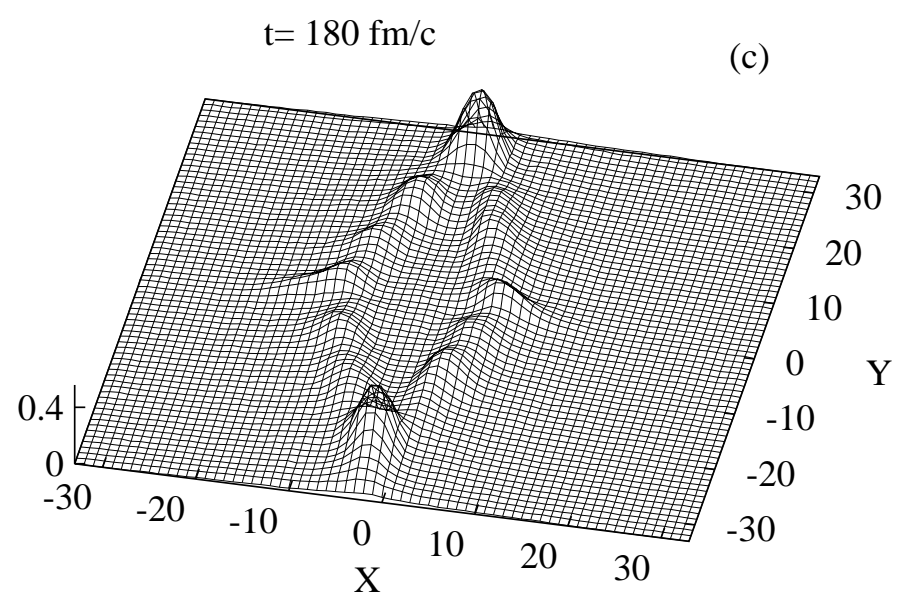


Fig.1

The sample average density profile $\langle \rho(x, y; t) \rangle / \rho_0$ versus the position (x, y) is shown for different times.

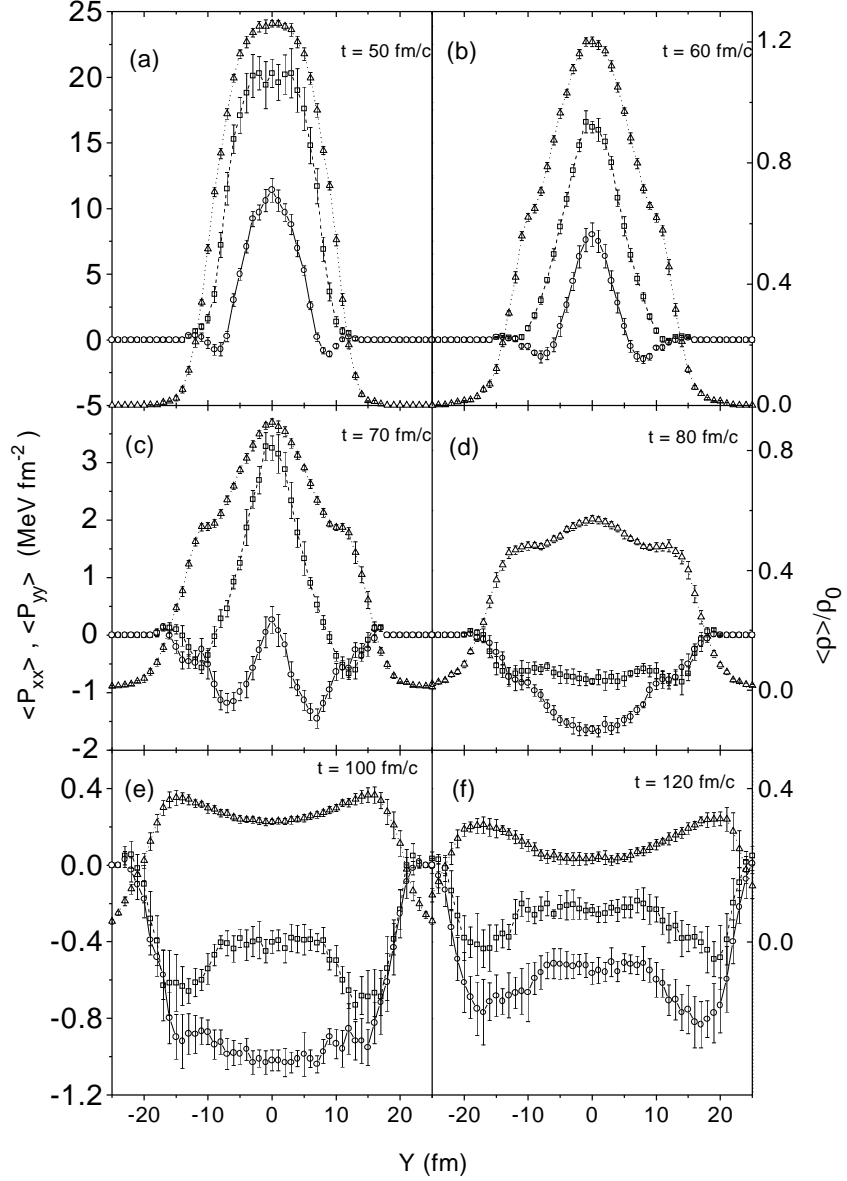


Fig. 2

The sample averaged values of the diagonal components of pressure tensor, $\langle P_{xx} \rangle$ and $\langle P_{yy} \rangle$ along y axis are shown by squares and circles, respectively for different time steps indicated in the figure. The sample averaged value of density $\langle \rho \rangle$ in units of ρ_0 along the y axis also shown by triangles in the same graph. The sample fluctuations are indicated by the error bars. The curves connecting the points are to guide the eye.

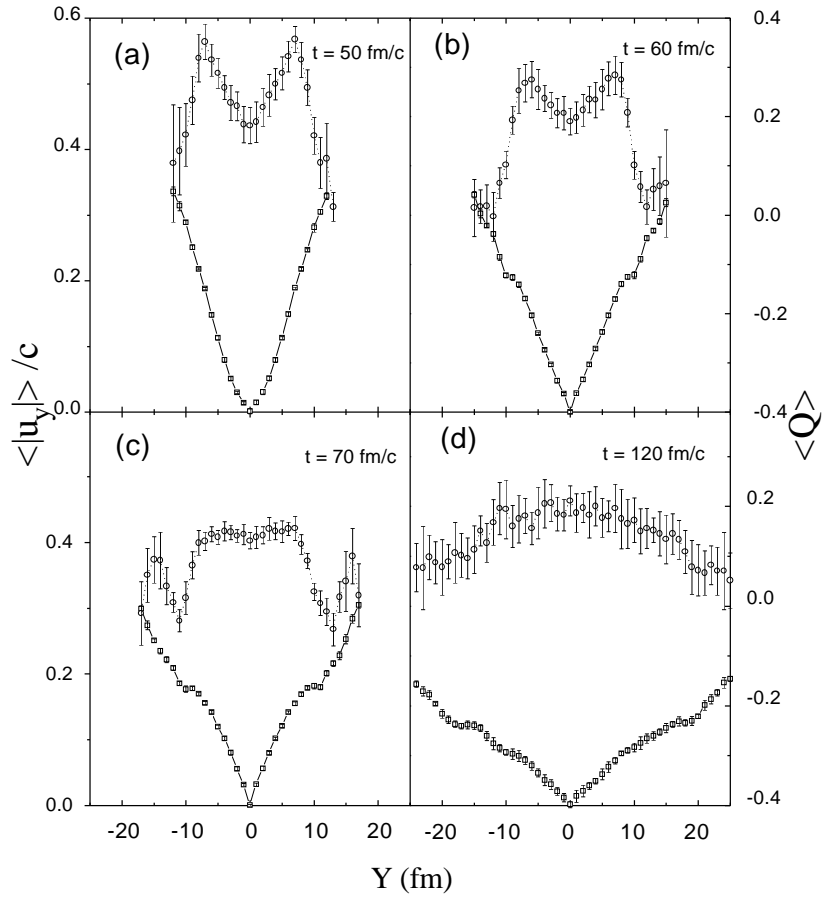


Fig. 3

The sample averaged values of the magnitude of the y component of flow velocity $\langle |u_y| \rangle$ along y axis are shown by squares for different time steps. The sample averaged values of the asymmetry variable $\langle Q \rangle$ along the y axis also shown by circles in the same graph. The sample fluctuations are indicated by the error bars. The curves connecting the points are to guide the eye.

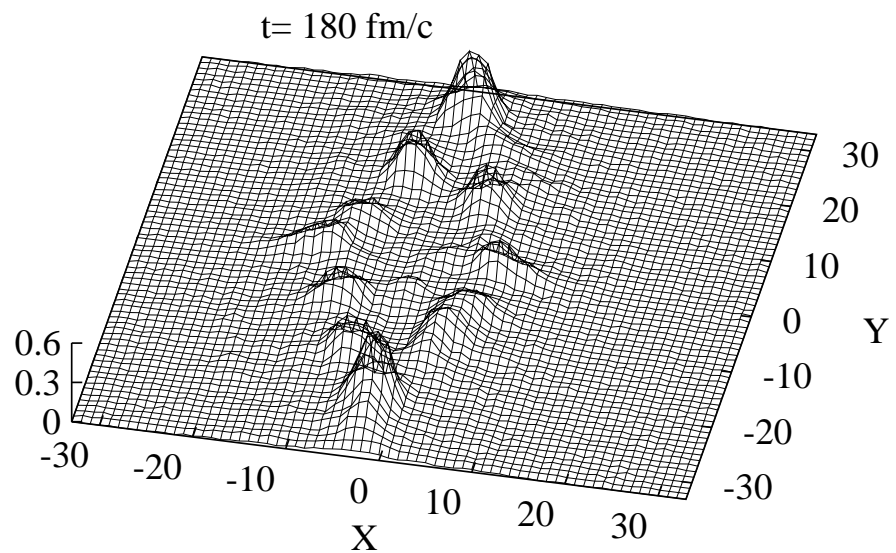


Fig. 4

The density profile $\rho(x, y; t)/\rho_0$ versus the position (x, y) for a particular sample is shown. The angles of view are same as that of Fig. 1.